# Short Pauses in Thalamic Deep Brain Stimulation Promote Tremor and Neuronal Bursting

**Brandon D. Swan**[a], **David T. Brocker**[a], **Justin D. Hilliard**[a], **Stephen B. Tatter**[b], **Robert E. Gross**[c], **Dennis A. Turner**[d,e], and **Warren M. Grill**[a,d,e,f,*]

[a]Department of Biomedical Engineering, Duke University, Durham, NC, USA

[b]Department of Neurosurgery, Wake Forest University Baptist Medical Center, Winston-Salem, NC, USA

[c]Departments of Neurosurgery and Neurology, Emory University School of Medicine, Atlanta, GA, USA

[d]Department of Surgery, Duke University Medical Center, Durham, NC, USA

[e]Department of Neurobiology, Duke University Medical Center, Durham, NC, USA

[f]Department of Electrical and Computer Engineering, Duke University, Durham, NC, USA

## Abstract

**Objective**—We conducted intraoperative measurements of tremor during DBS containing short pauses ( 50 ms) to determine if there is a minimum pause duration that preserves tremor suppression.

**Methods**—Nine subjects with ET and thalamic DBS participated during IPG replacement surgery. Patterns of DBS included regular 130 Hz stimulation interrupted by 0, 15, 25 or 50 ms pauses. The same patterns were applied to a model of the thalamic network to quantify effects of pauses on activity of model neurons.

**Results**—All patterns of DBS decreased tremor relative to 'off'. Patterns with pauses generated less tremor reduction than regular high frequency DBS. The model revealed that rhythmic burst-driver inputs to thalamus were masked during DBS, but pauses in stimulation allowed propagation of bursting activity. The mean firing rate of bursting-type model neurons as well as the firing pattern entropy of model neurons were both strongly correlated with tremor power across stimulation conditions.

*Corresponding Author: W.M. Grill, Duke University, Department of Biomedical Engineering, Hudson Hall, Rm 136, Box 90281, Durham NC 27708-0281, USA, Tel.: +1 919 660 5276, Fax: +1 919 684 4488, warren.grill@duke.edu.

**Conflict of Interest**

**Conclusion—**The temporal pattern of stimulation influences the efficacy of thalamic DBS. Pauses in stimulation resulted in decreased tremor suppression indicating that masking of pathological bursting is a mechanism of thalamic DBS for tremor.

**Significance—**Pauses in stimulation decreased the efficacy of open-loop DBS for suppression of tremor.

### Keywords

Essential tremor; movement disorders; thalamus; deep brain stimulation; computational model

## 1. Introduction

Thalamic deep brain stimulation (DBS) is an effective therapy for treatment of essential tremor, but the neural mechanisms of action underpinning its efficacy are not well understood. The effects of DBS are strongly dependent on stimulation frequency; high frequency (> 100 Hz) DBS alleviates postural tremor [Kuncel et al., 2006; Sydow et al., 2003], whereas low frequency DBS is clinically ineffective and may exacerbate tremor [Cagnan et al., 2013; Pedrosa et al., 2013]. Therapeutic efficacy is also sensitive to the temporal pattern of stimulation [Birdno et al., 2007, 2008; Brocker et al., 2013; Dorval et al., 2010; Montgomery et al., 2005] and increasing evidence suggests that long pauses during stimulation ( 50 ms) reduce tremor suppression during Vim thalamic DBS [Birdno et al., 2012; Kuncel et al., 2012]. Pauses during stimulation can lead to rebound burst firing in thalamic neurons following a release from inhibition, mediated by a T-Type $Ca^{2+}$ current [Jahnsen and Llinás, 1984; Person and Perkel, 2005], and this phenomenon is hypothesized to exacerbate tremor.

In this study we measured responses to patterns of thalamic DBS with short pauses ( 50 ms) in human subjects with essential tremor (ET) and in a validated biophysical network model of ventral thalamus [Birdno et al., 2012] to determine if there is a critical pause duration for tremor suppression. Results from clinical and computational studies indicate that short pauses in stimulation trains decrease DBS effectiveness and enable propagation of pathological bursting activity in the cerebello-thalamocortical pathway. In the absence of pauses, stimulation masked burst activity and regularized firing patterns in the thalamic network model. These results suggest that activation of cerebellar afferent inputs to the thalamus mediates the therapeutic effects of DBS, and provide the groundwork for development of improved temporally-patterned stimulation to treat postural tremor in persons with ET.

## 2. Methods

We measured postural tremor during temporal patterns of high frequency stimulation with short pauses (15-50 ms) in human subjects with ET and DBS in the ventral intermediate nucleus (Vim) of the thalamus. The effects of the same patterns on neuronal firing patterns were quantified in a computational model of the Vim thalamic network.

### 2.1. Human Subjects Enrollment

We recruited patients with Vim thalamic DBS for ET undergoing elective implantable pulse generator (IPG) replacement surgery at Duke University Medical Center, Emory University Hospital, and Wake Forest Baptist Medical Center. The study protocol was reviewed and approved by the respective Institutional Review Boards prior to study initiation. Candidate subjects were screened for inclusion at least three months following DBS electrode implant or revision. All participants were capable of performing a postural tremor assessment task, neurologically stable, and capable of understanding the study and consent form. Subjects participated on a volunteer basis and provided written informed consent prior to enrollment. Nine subjects completed at least two of the three randomized blocks of the study protocol and were included in data analysis.

### 2.2. Intraoperative Setup

Intraoperative studies were conducted using methods previously described [Swan et al., 2014], and briefly summarized below.

Subjects withheld anti-tremor medications for at least 12 hours prior to surgery. Preoperative and intraoperative sedatives were not administered until the research measurements were complete. Subjects were positioned comfortably supine, prepared and draped with one arm fully exposed and mobile to facilitate interaction with the experimenters. A triaxial accelerometer (CXL04LP3, Crossbow; San Jose, CA) was fixed to the dorsum of the hand to measure tremor responses during the experiment. The depleted IPG was then explanted under local and monitored anesthesia care. The exposed DBS extension cable was connected to an external stimulator outside the sterile field via a sterile adapter (1×4 Pocket Adaptor for Deep Brain Stimulation, #64001; Medtronic Inc., Minneapolis, MN), extension cable (Multi-lead Trailing Cable, #355531; Medtronic Inc.), and a custom extension cable.

An optical stimulus isolator (bp Isolator; FHC Inc., Bowdoinham, ME) connected to a laptop-controlled, isolated multifunction data acquisition device (USB-6216 BNC; National Instruments, Austin, TX) delivered unilateral stimulation to the electrode implanted contralateral to the arm used for tremor measurement. Charge-balanced, biphasic, regulated voltage pulses similar to those produced by the clinical IPG were used to deliver temporal patterns of stimulation generated by custom software (LabVIEW; National Instruments, Austin, TX). Clinically programmed values for all other stimulation parameters were replicated when possible (Table 1). Subjects with monopolar stimulation contact configurations were switched to bipolar configurations by changing stimulation return to a clinically unused contact (2/9 subjects). Some subjects experienced discomfort in response to intraoperative stimulation at the clinically programmed stimulation amplitude, and the voltage was decreased to the maximum tolerable level for these individuals (3/9 subjects). IPGs near end-of-life often require an increased stimulation amplitude to compensate for lower current output due to decreased battery supply voltage [Montuno et al., 2013]. Therefore, intraoperative stimulation at the clinically programmed voltage may have caused discomfort due to delivery of more current than the depleted IPG produced. Some subjects experienced paresthesias in response to stimulation, but these were not reported as

uncomfortable. Stimulation amplitude was increased above the clinical level for one subject to improve tremor control. There were no adverse events during this study.

### 2.3. Stimulation Pattern Design

We measured tremor during temporal patterns of high frequency DBS with short pauses, high frequency DBS without pauses, and the DBS off condition (Figure 1a). Stimulation patterns with pauses were comprised of constant-frequency pulse trains periodically interrupted by periods of no stimulation. Pauses of 15, 25, or 50 ms occurred at a rate of 4.4 Hz in three of these patterns, consistent with the primary tremor frequency in ET patients [Deuschl, et al., 1998], and 50 ms pauses occurred at 2.2 Hz in another pattern. The interpulse intervals of pulse trains between pauses were constant within each pattern, but varied between stimulation patterns such that the geometric mean frequency for all patterns was 130 Hz. Pauses decreased the total percentage of time that pulses were delivered by 6.6%, 11.0%, or 22.0% relative to constant 130 Hz stimulation.

### 2.4. Experiment Protocol

Stimulation patterns were presented in a randomized block design and subjects were blinded to the stimulation pattern (Figure 1b). Each trial consisted of a 60 s epoch with stimulation off (*Pre* trial period), followed by a 60 s epoch with one of the six stimulation conditions (five DBS patterns and DBS OFF). Postural tremor was measured for 20 s starting midway through each trial with the subject's arm in the position that maximized tremor amplitude. After each stimulation condition was evaluated, the order of stimulation conditions was re-randomized and subjects completed one additional block (1/9 subjects) or two additional blocks (8/9 subjects) of trials. Following completion of the experimental protocol, the DBS extension was disconnected from the research equipment and the IPG replacement procedure continued according to normal care.

### 2.5. Computational Modeling

We used a biophysically based computational network model of the ventral motor thalamus to simulate the responses of thalamocortical (TC) neurons to the same DBS patterns that were delivered intraoperatively [Birdno et al., 2012]. This model was comprised of 50 TC relay neurons [McIntyre et al., 2004], each receiving terminating axons from cerebellum (CER), cortex (CTX), reticular nucleus (RN) and local thalamic interneurons (TINs) [Darian-Smith et al., 1996; Tasker and Kiss, 1995] (Figure 2a). The strengths of GABAergic synapses from RN and TINs to TC neurons were varied to reproduce three classes of TC neuron response types in the proportions they are observed in humans with ET (~50% bursting, ~30% regular-spiking, and ~20% random-spiking) [Molnar et al., 2005]. Intrinsic activity of CER fibers was modeled after activity recorded in the harmaline model of tremor in cats [de Montigny and Lamarre, 1973].

These inputs delivered bursts of spike trains at a rate of 5.8 Hz, which is the predominant interburst frequency of Vim neurons in humans with ET [Hua and Lenz, 2005]. Cortical inputs were generated using a 20 Hz Poison process [Deschênes and Hu, 1990]. Synaptic excitation of the RN by CTX inputs and feedback from TC neuron output generated RN

activity [Ando et al., 1995; Steriade et al., 1997]. Inhibitory local TIN activity resulted from synaptic excitation from CTX and CER inputs [Ando et al., 1995].

We calculated the extracellular voltages generated by DBS using a finite element model (COMSOL, Burlilngton, MA). We modeled the ventral motor thalamus as an oblique rectangular prism with TC cell bodies randomly positioned in this volume (Figure 2b). The axons of these cells were oriented along a straight trajectory from the center of the inferior base of Vim thalamus to the hand area of primary cortex [Hlustík et al., 2001]. Cortical axons followed an inversely symmetric trajectory to TC axons, CER axons were oriented 30° posterior to the coronal plane, and the RN and TIN axons extended in the lateral-medial and medial-lateral directions, respectively. We situated this prism within an 8,000 cm$^3$ cube with the border set to 0 V to approximate monopolar cathodic stimulation with the implanted pulse generator as the return electrode. The tissue was modeled as a homogenous isotropic medium with a conductivity of 0.2 S/m.

The most ventral electrode, contact 0, of a Medtronic DBS lead (Model 3387, Minneapolis, MN) was positioned in the center of Vim thalamus and oriented 30° anterior to the coronal plane [Mobin et al., 1999], although the optimal location for tremor control is at the ventral border of Vim thalamus, near cerebellar fibers [Klein et al., 2012]. The conductivities of the metal electrodes and insulating material between electrodes were 1e7 and 1e-10 S/m, respectively [Wei and Grill, 2005]. The surface of contact 0 was set to a constant voltage boundary condition, and continuity of current density normal to the surface was imposed at all other components of the DBS lead.

We implemented model neurons in Neuron 6.1 [Hines and Carnevale, 1997], using backwards Euler integration with a time step of 10 μs to obtain the transmembrane potential in response to DBS. Simulations were run for 14 s each, consisting of 10 s of stimulation, preceded and followed by 2 s periods without stimulation that were excluded from subsequent model analysis. The stimulation amplitude was set to 7.5V, which was sufficient to activate directly 32 of the 50 TC neurons in the absence of other inputs. This amplitude is high relative to typical clinical values, and is a reflection of the relatively low density of modeled TC neurons simulated in our model. We chose this amplitude to activate a sufficient number of neurons, as changes in tremor suppression are strongly correlated with changes in the proportion of activated neurons across varying stimulation voltages [Kuncel et al., 2007].

## 2.6. Data Analysis and Statistics

Tremor amplitudes measured by accelerometry correlate well with clinical tremor ratings [Elble et al., 2006]. We sampled the x-, y-, and z-axis signals from a triaxial accelerometer at 1000 Hz during tremor measurement epochs using custom Labview software (LabVIEW; National Instruments, Austin, TX). The recorded voltages were converted to acceleration using appropriate calibration parameters [Lueck and Wolk, 2002]. To quantify tremor severity we performed spectral analysis of the acceleration signals (power spectral density, Welch's averaged periodogram, Hanning window, fast Fourier Transform (FFT) length = 5000) in MATLAB (MathWorks; Natick, MA) (Figure 3). These spectra were summed across all three axes then integrated from 1-20 Hz to obtain tremor power; this range spans

the typical frequency range of tremor and its major harmonics [Pahwa and Lyons, 2003]. Tremor severity was analyzed as the log-transform of tremor power. Statistical differences in tremor severity across stimulation conditions were analyzed using a linear mixed-effects model with stimulation condition as a fixed effect and subject identity as a random effect. Tremor measurements made during *Pre* trials were excluded from this analysis to prevent possible carryover effects caused by preceding stimulation epochs.

Average spike train entropy was calculated to quantify the irregularity of the model neuron firing patterns as this measure correlates well with the efficacy of DBS in treating the symptoms of movement disorders in humans [Dorval et al., 2010; Kuncel et al., 2012] and non-human primates [Dorval et al., 2008]. We calculated the first order estimate of entropy (*H*) for log-transformed interspike intervals (ISIs) of all model TC neurons as:

$$H \quad = \quad -\sum_{i=1}^{250} p\left(\log ISI_i\right) \log_2\left(\log ISI_i\right)$$

where $p(\log ISI_i)$ represents the proportion of the total ISIs in bin *i*, where bins range from 0.6 to 10,000 ms in 250 logarithmically-distributed bins (bin width = 0.017 log ms). Differences in spike train entropy across stimulation conditions were analyzed using a repeated measures analysis of variance (ANOVA), using entropy as the repeated measure. Statistical models were implemented in JMP 10 Pro for Mac OS X (SAS Institute, Inc.; Cary, NC). Tukey's honestly significant difference (HSD) test was used to make post hoc comparisons of entropy and tremor across stimulation conditions. The residuals of the entropy and log-transformed tremor measures were normally distributed (visual inspection of the residual normality (Q-Q) plot). Statistical significance was defined at $\alpha = 0.05$.

## 3. Results

### 3.1. Tremor Responses to Pause Patterns

We measured postural tremor responses in nine subjects with Vim DBS during high frequency stimulation with short pauses. Tremor severity was quantified using log-transformed tremor power during four stimulation patterns with pauses (15, 25, or 50 ms at 4.4z; 50ms at 2.2 Hz), constant-frequency stimulation (130 Hz) and stimulation off (Figure 4). Although the geometric mean frequency of all stimulation patterns was held constant, tremor varied across stimulation patterns (F = 18.8, p<0.0001, linear mixed-effects model). All stimulation patterns reduced tremor relative to the stimulation off condition (p<0.0001, Tukey's HSD). Constant frequency stimulation without pauses provided the greatest reduction of tremor relative to the off condition (p<0.0001, Tukey's HSD), as in previous reports on DBS with pauses [Birdno et al., 2012; Kuncel et al., 2012]. Stimulation with all pause patterns was less effective than stimulation without pauses, but 15 ms pause patterns did not produce statistically different tremor reduction than continuous DBS (p = 0.077, Tukey's HSD).

### 3.2. Model Responses to Pause Patterns

We simulated the activity of model neurons in a Vim thalamic network model in response to the same DBS patterns tested clinically. Example somatic activity of model TC neurons is shown in Figure 5, with representative neuron sub-types selected in proportion to their representation in humans with ET (three regular-spiking, two random-spiking, and five bursting-type). In the absence of DBS, burst type neurons fired bursts of spikes between periods of afferent cerebellar activity due to release from TIN-mediated inhibition, whereas regular- and random-spiking neurons fired continuously (Figure 5b). Application of 130 Hz constant-frequency DBS increased somatic firing in random-spiking neurons, increased or decreased somatic firing in regular-spiking neurons, and silenced somatic activity in bursting-type neurons (Figure 5a).

Somatic responses to DBS with pauses were similar to those in response to 130 Hz constant-frequency DBS in regular-spiking and random-spiking TC neurons (Figure 6a,c). However, some bursting-type neurons fired somatic bursts during pauses in afferent cerebellar bursting activity that were coincident with pauses in stimulation, and these bursts led to axonal burst firing during pauses (Figure 6b,d). Conversely, somatic firing in burst type cells was inhibited during periods of stimulation (between pauses), and during periods of bursting cerebellar afferent activity, regardless of whether they were coincident. The somatic firing rate of burst type neurons varied with stimulation pattern, with longer pauses permitting more burst firing (F = 17.5, p<0.0001, ANOVA). Mean somatic firing rate of burst-type model neurons correlated well with mean log-transformed tremor power ($R^2$=0.733) (Figure 7).

We quantified the regularity of TC neuron axon firing by calculating the first order entropy of log-transformed interspike intervals [Dorval 2008]. Firing pattern entropy averaged across all neurons was dependent on stimulation pattern (F = 37.8, p <0.0001, ANOVA) (Figure 8a). Compared to the off condition, all patterns of stimulation significantly reduced entropy (p<0.001, Tukey's HSD). Constant frequency stimulation significantly reduced entropy more than stimulation with 25 and 50 ms pauses (p<0.020, Tukey's HSD), but not 15 ms pause patterns (p=0.12, Tukey's HSD). These changes in neural firing pattern paralleled the changes in mean log-transformed tremor power across stimulation patterns, and there was a very strong correlation between these measures ($R^2$=0.93) (Figure 8b).

Within sub-types of TC neurons, stimulation reduced entropy relative to the off condition in almost all cases (p=0.056 for stimulation with 50 ms pauses at 4.4Hz of random-spiking type; p<0.047 all other cases, Tukey's HSD), but only bursting-type neurons showed significant differences between constant frequency stimulation and pause patterns. Constant frequency stimulation reduced bursting-type entropy relative to 25 and 50 ms pause patterns (p<0.0006, Tukey's HSD). Stimulation with 15 ms pauses reduced bursting-type entropy more than stimulation with 50 ms pauses at a rate of 4.4 Hz (p=0.002, Tukey's HSD), but not more than constant frequency stimulation (p=0.092, Tukey's HSD).

## 4. Discussion

We measured postural tremor in human subjects during DBS with patterns containing short (15-50 ms) pauses to determine if there is a critical pause duration that leads to a reduction of tremor control. Constant frequency stimulation suppressed tremor more than stimulation with 25 or 50 ms pauses, while tremor suppression with DBS containing 15 ms pauses was not statistically different than continuous stimulation, and there were no significant differences in tremor power between pause trains. The same patterns of DBS were applied to a computational model of the Vim thalamic network to investigate the neural correlates of tremor during DBS. DBS with pauses increased firing pattern entropy in model thalamocortical neurons and somatic firing rate in burst-type model neurons, as compared to continuous DBS. These outcomes were strongly correlated with clinical tremor measures, and reinforce the previous finding that DBS suppresses tremor by masking bursting activity carried by cerebellar inputs to the thalamus via activation of pre-synaptic cerebellar fibers [Birdno et al., 2012].

High frequency DBS ameliorates the symptoms of movement disorders, and varying the temporal pattern of stimulation can cause therapeutic efficacy to decrease, even when stimulation is delivered at a high average frequency [Birdno et al., 2007; Birdno et al., 2008; Dorval et al., 2010; Montgomery, 2005]. For example, longer pauses in stimulation trains ( 50 ms) result in decreased postural tremor control in response to irregular Vim thalamic DBS [Birdno et al., 2012; Kuncel et al., 2012]. We performed clinical experiments to determine whether short pauses during high frequency thalamic DBS ( 50 ms) modulate the severity of essential tremor. All stimulation patterns reduced tremor from the baseline DBS off condition. Although these patterns maintained the same geometric mean frequency, only stimulation with 15 ms pauses occurring at 4.4 Hz was not significantly worse than constant-frequency stimulation without pauses. This finding confirms that pauses, as short in duration as 25 ms, can adversely affect the performance of DBS for treatment of tremor.

Pathological single-unit bursting activity recorded in human thalamus has been implicated in the genesis of tremor in patients with ET [Hua and Lenz, 2005; Kobayashi et al., 2003; Lee et al., 2003; Lenz et al., 1994; Molnar et al., 2005]. Thalamic bursting in the computational model was driven by cerebellar inputs transmitting oscillatory burst activity at the predominant interburst frequency of Vim neurons in humans with ET [Hua and Lenz, 2005]. This pathological activity generated high firing pattern entropy in model TC cells during the no DBS condition. Stimulation with all patterns significantly reduced entropy, particularly in bursting-type cells, but entropy increased with increasing pause duration. Longer pauses also permitted more bursting activity in these cells when pauses in stimulation coincided with pauses in bursting activity of cerebellar inputs. Changes in entropy and somatic burst firing were highly correlated with tremor in human subjects, reinforcing the hypothesis that DBS alleviates motor symptoms by masking pathological activity via regularization of neuronal firing [Grill et al., 2004]. These results are also consistent with other studies suggesting that optimal tremor attenuation is achieved through activation of afferent cerebellar fibers by stimulation of the posterior subthalamic area [Blomstedt et al., 2010; Coenen et al., 2011].

Thalamic bursting may be generated *in vitro* following release from hyperpolarization through a rebound mechanism mediated by the T-type $Ca^{2+}$ current [Jahnsen and Llinás, 1984]. Pauses in thalamic stimulation lasting ~25 ms or longer generate rebound burst events *in vivo* [Person and Perkel, 2005], and propagation of this bursting activity through the thalamocortical circuit is thought to exacerbate tremor. Stimulation patterns tested in the present study included pulse trains with pauses of durations less than, equal to, or greater than this threshold (15, 25, or 50 ms, respectively). However, tremor severity did not significantly differ between any of pause patterns tested. This result, coupled with the occurrence of burst-type somatic firing during pauses of all tested durations, suggests that bursting activity following short pauses in stimulation may result from propagation of driven burst activity arising from cerebellum, rather than a local rebound burst mechanism.

The stimulation patterns delivered pauses in DBS in an open-loop fashion, independent of the phase of tremor or neural oscillations in the thalamic network. However, the finding that burst responses in the model occurred only during simultaneous pauses in DBS and cerebellar input activity highlights the importance of the interaction between the temporal characteristics of applied stimulation and underlying pathological neural activity. Recent work in patients with ET showed that the effects of thalamic low-frequency DBS were dependent on the phase of the postural tremor cycle when individual pulses were delivered [Cagnan et al., 2013]. Additionally, experiments in a 1-methyl-4-phenyl-1,2,3,6-tetrahydropyridine (MPTP) model of Parkinson's disease showed that closed-loop stimulation triggered by a reference neural signal provided better symptom suppression than open-loop, constant-frequency DBS [Rosin et al., 2011]. We therefore tested in our model cycling patterns of DBS triggered to align with either the beginning or end of pauses in afferent cerebellar activity. Stimulation delivered only during pauses in cerebellar input generated suppression of somatic firing in burst-type neurons equal to that of constant frequency stimulation (Figure 9a), whereas stimulation between pauses did not (Figure 9b). Measurement of activity within the cerebello-thalamocortical pathway may provide the means for selective, on-demand therapeutic relief of tremor symptoms.

## 5. Conclusion

Pauses in stimulation decreased the efficacy of open-loop, high frequency DBS for suppression of tremor. Quantitative measures of neural activity correlated strongly with clinical tremor outcomes. Bursting activity of TC neurons was masked by regularization of firing patterns and reduction of bursting during DBS in a network thalamic model. The length of pauses during DBS and their timing relative to ongoing pathological bursting determines the ability of temporally irregular stimulation patterns to mask rebound bursting and thereby suppress tremor.

## Acknowledgements

# References

Ando N, Izawa Y, Shinoda Y. Relative contributions of thalamic reticular nucleus neurons and intrinsic interneurons to inhibition of thalamic neurons projecting to the motor cortex. J Neurophysiol. 1995; 73:2470–85. [PubMed: 7666153]

Birdno MJ, Cooper SE, Rezai AR, Grill WM. Pulse-to-pulse changes in the frequency of deep brain stimulation affect tremor and modeled neuronal activity. J Neurophysiol. 2007; 98:1675–84. [PubMed: 17634335]

Birdno MJ, Kuncel AM, Dorval AD, Turner DA, Grill WM. Tremor varies as a function of the temporal regularity of deep brain stimulation. Neuroreport. 2008; 19:599–602. [PubMed: 18388746]

Birdno MJ, Kuncel AM, Dorval AD, Turner DA, Gross RE, Grill WM. Stimulus features underlying reduced tremor suppression with temporally patterned deep brain stimulation. J Neurophysiol. 2012; 107:364–83. [PubMed: 21994263]

Blomstedt P, Sandvik U, Tisch S. Deep brain stimulation in the posterior subthalamic area in the treatment of essential tremor. Mov Disord. 2010; 25:1350–6. [PubMed: 20544817]

Brocker DT, Swan BD, Turner DA, Gross RE, Tatter SB, Koop MM, et al. Improved efficacy of temporally non-regular deep brain stimulation in Parkinson's disease. Exp Neurol. 2013; 239:60–7. [PubMed: 23022917]

Cagnan H, Brittain JS, Little S, Foltynie T, Limousin P, Zrinzo L, et al. Phase dependent modulation of tremor amplitude in essential tremor through thalamic stimulation. Brain. 2013; 136:3062–75. [PubMed: 24038075]

Coenen VA, Mädler B, Schiffbauer H, Urbach H, Allert N. Individual fiber anatomy of the subthalamic region revealed with diffusion tensor imaging: a concept to identify the deep brain stimulation target for tremor suppression. Neurosurgery. 2011; 68:1069–75. discussion 1075-6. [PubMed: 21242831]

Darian-Smith I, Galea MP, Darian-Smith C, Sugitani M, Tan A, Burman K. The anatomy of manual dexterity. The new connectivity of the primate sensorimotor thalamus and cerebral cortex. Adv Anat Embryol Cell Biol. 1996; 133:1–140. [PubMed: 8854379]

de Montigny C, Lamarre Y. Rhythmic activity induced by harmaline in the olivo-cerebello-bulbar system of the cat. Brain Res. 1973; 53:81–95. [PubMed: 4697252]

Deschênes M, Hu B. Electrophysiology and Pharmacology of the Corticothalamic Input to Lateral Thalamic Nuclei: an Intracellular Study in the Cat. Eur J Neurosci. 1990; 2:140–152. [PubMed: 12106057]

Deuschl G, Bain P, Brin M. Consensus statement of the Movement Disorder Society on Tremor. Ad Hoc Scientific Committee. Mov Disord. 1998; 13(Suppl 3):2–23. [PubMed: 9827589]

Dorval AD. Probability distributions of the logarithm of inter-spike intervals yield accurate entropy estimates from small datasets. J Neurosci Methods. 2008; 173:129–39. [PubMed: 18620755]

Dorval AD, Russo GS, Hashimoto T, Xu W, Grill WM, Vitek JL. Deep brain stimulation reduces neuronal entropy in the MPTP-primate model of Parkinson's disease. J Neurophysiol. 2008; 100:2807–18. [PubMed: 18784271]

Dorval AD, Kuncel AM, Birdno MJ, Turner DA, Grill WM. Deep brain stimulation alleviates parkinsonian bradykinesia by regularizing pallidal activity. J Neurophysiol. 2010; 104:911–21. [PubMed: 20505125]

Elble RJ, Pullman SL, Matsumoto JY, Raethjen J, Deuschl G, Tintner R, Tremor Research Group. Tremor amplitude is logarithmically related to 4- and 5-point tremor rating scales. Brain. 2006; 129:2660–6. [PubMed: 16891320]

Grill WM, Snyder AN, Miocinovic S. Deep brain stimulation creates an informational lesion of the stimulated nucleus. Neuroreport. 2004; 15:1137–40. [PubMed: 15129161]

Hines ML, Carnevale NT. The NEURON simulation environment. Neural Comput. 1997; 9:1179–209. [PubMed: 9248061]

Hlustík P, Solodkin A, Gullapalli RP, Noll DC, Small SL. Somatotopy in human primary motor and somatosensory hand representations revisited. Cereb Cortex. 2001; 11:312–21. [PubMed: 11278194]

Hua SE, Lenz FA. Posture-related oscillations in human cerebellar thalamus in essential tremor are enabled by voluntary motor circuits. J Neurophysiol. 2005; 93:117–27. [PubMed: 15317839]

Jahnsen H, Llinás R. Voltage-dependent burst-to-tonic switching of thalamic cell activity: an in vitro study. Arch Ital Biol. 1984; 122:73–82. [PubMed: 6087765]

Klein JC, Barbe MT, Seifried C, Baudrexel S, Runge M, Maarouf M, et al. The tremor network targeted by successful VIM deep brain stimulation in humans. Neurology. 2012; 78:787–95. [PubMed: 22377809]

Kobayashi K, Katayama Y, Kasai M, Oshima H, Fukaya C, Yamamoto T. Localization of thalamic cells with tremor-frequency activity in Parkinson's disease and essential tremor. Acta Neurochir Suppl. 2003; 87:137–9. [PubMed: 14518541]

Kuncel AM, Cooper SE, Wolgamuth BR, Clyde MA, Snyder SA, Montgomery EB Jr, et al. Clinical response to varying the stimulus parameters in deep brain stimulation for essential tremor. Mov Disord. 2006; 21:1920–8. [PubMed: 16972236]

Kuncel AM, Cooper SE, Wolgamuth BR, Grill WM. Amplitude- and frequency-dependent changes in neuronal regularity parallel changes in tremor with thalamic deep brain stimulation. IEEE Trans Neural Syst Rehabil Eng. 2007; 15:190–7. [PubMed: 17601188]

Kuncel AM, Birdno MJ, Swan BD, Grill WM. Tremor reduction and modeled neural activity during cycling thalamic deep brain stimulation. Clin Neurophysiol. 2012; 123:1044–52. [PubMed: 21978653]

Lee BH, Lee KH, Chung SS, Chang JW. Neurophysiological identification and characterization of thalamic neurons with single unit recording in essential tremor patients. Acta Neurochir Suppl. 2003; 87:133–6. [PubMed: 14518540]

Lenz FA, Kwan HC, Martin RL, Tasker RR, Dostrovsky JO, Lenz YE. Single unit analysis of the human ventral thalamic nuclear group. Tremor-related activity in functionally identified cells. Brain. 1994; 117:531–43. [PubMed: 8032863]

Lueck R, Wolk F. A Quick Method for Calibrating Accelerometers. 2002 Rockland Sci. Intl. Inc., Victoria, B.C., Canada, Tech Note TN-001.

McIntyre CC, Grill WM, Sherman DL, Thakor NV. Cellular effects of deep brain stimulation: model-based analysis of activation and inhibition. J Neurophysiol. 2004; 91:1457–69. [PubMed: 14668299]

Mobin F, De Salles AA, Behnke EJ, Frysinger R. Correlation between MRI-based stereotactic thalamic deep brain stimulation electrode placement, macroelectrode stimulation and clinical response to tremor control. Stereotact Funct Neurosurg. 1999; 72:225–32. [PubMed: 10853082]

Molnar GF, Pilliar A, Lozano AM, Dostrovsky JO. Differences in neuronal firing rates in pallidal and cerebellar receiving areas of thalamus in patients with Parkinson's disease, essential tremor, and pain. J Neurophysiol. 2005; 93:3094–101. [PubMed: 15703231]

Montgomery EB Jr. Effect of subthalamic nucleus stimulation patterns on motor performance in Parkinson's disease. Parkinsonism Relat Disord. 2005; 11:167–71. [PubMed: 15823481]

Montuno MA, Kohner AB, Foote KD, Okun MS. An algorithm for management of deep brain stimulation battery replacements: devising a web-based battery estimator and clinical symptom approach. Neuromodulation. 2013; 16:147–53. [PubMed: 22646907]

Pahwa R, Lyons KE. Essential tremor: differential diagnosis and current therapy. Am J Med. 2003; 115:134–42. [PubMed: 12893400]

Pedrosa DJ, Auth M, Eggers C, Timmermann L. Effects of low-frequency thalamic deep brain stimulation in essential tremor patients. Exp Neurol. 2013; 248:205–12. [PubMed: 23778146]

Person AL, Perkel DJ. Unitary IPSPs drive precise thalamic spiking in a circuit required for learning. Neuron. 2005; 46:129–40. [PubMed: 15820699]

Rosin B, Slovik M, Mitelman R, Rivlin-Etzion M, Haber SN, Israel Z, et al. Closed-loop deep brain stimulation is superior in ameliorating parkinsonism. Neuron. 2011; 72:370–84. [PubMed: 22017994]

Steriade, M.; Jones, EG.; McCormick, DA. Thalamus. Vol. 1. Elsevier Science Ltd; Oxford: 1997. p. 1700

Swan BD, Grill WM, Turner DA. Investigation of Deep Brain Stimulation Mechanisms During Implantable Pulse Generator Replacement Surgery. Neuromodulation. 2014; 17:419–24. [PubMed: 24118257]

Sydow O, Thobois S, Alesch F, Speelman JD. Multicentre European study of thalamic stimulation in essential tremor: a six year follow up. J Neurol Neurosurg Psychiatry. 2003; 74:1387–91. [PubMed: 14570831]

Tasker RR, Kiss ZH. The role of the thalamus in functional neurosurgery. Neurosurg Clin N Am. 1995; 6:73–104. [PubMed: 7696876]

Wei XF, Grill WM. Current density distributions, field distributions and impedance analysis of segmented deep brain stimulation electrodes. J Neural Eng. 2005; 2:139–47. [PubMed: 16317238]

## Highlights

- Pauses in thalamic DBS decreased tremor suppression relative to regular DBS in human subjects.

- Firing rate and entropy of model neurons in a thalamic network model correlated well with tremor power.

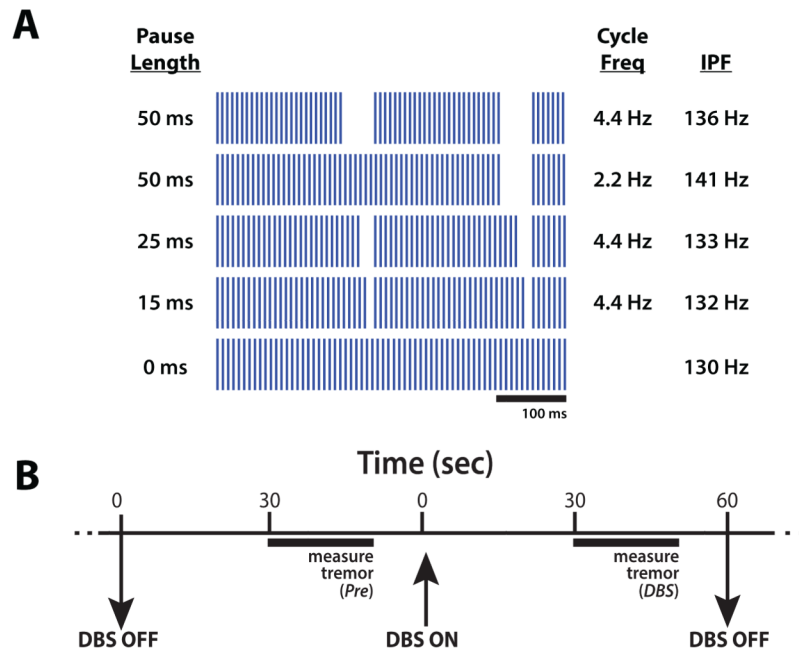- Pauses reduce thalamic DBS efficacy by preventing masking of pathological burst activity.

**A**

| Pause Length | | Cycle Freq | IPF |
|---|---|---|---|
| 50 ms | | 4.4 Hz | 136 Hz |
| 50 ms | | 2.2 Hz | 141 Hz |
| 25 ms | | 4.4 Hz | 133 Hz |
| 15 ms | | 4.4 Hz | 132 Hz |
| 0 ms | | | 130 Hz |

100 ms

**B**

Time (sec)

0     30     0     30     60

measure tremor (*Pre*)     measure tremor (*DBS*)

DBS OFF     DBS ON     DBS OFF

**Figure 1.**
Tremor was measured during temporal patterns of thalamic deep brain stimulation (DBS) containing short pauses. (A) Patterns of DBS, labeled with pause duration, frequency of pauses, and instantaneous pulse frequency (IPF) between pauses. All patterns had a geometric mean frequency of 130 Hz. (B) Timeline of intraoperative trials to measure tremor. Twenty-second measurements of tremor were made following thirty seconds without stimulation (*Pre*), and again after thirty seconds with one of the stimulation patterns in (A) or DBS OFF.
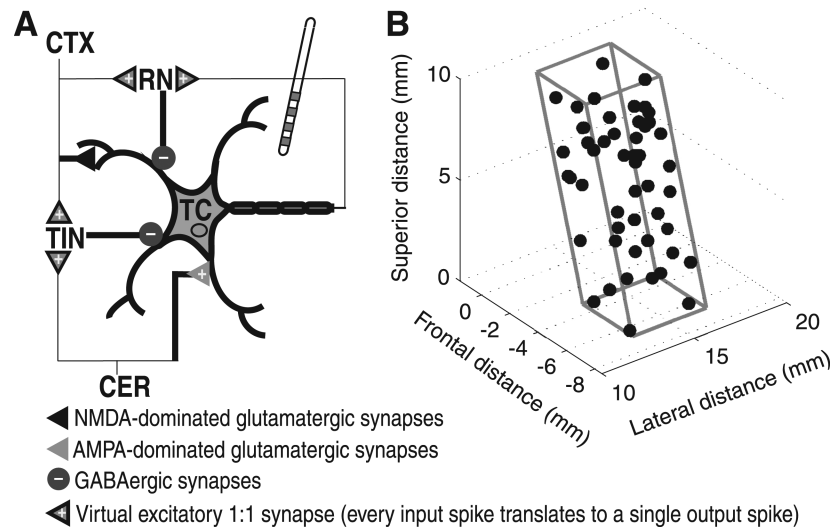
**Figure 2.**
Computational model of thalamic DBS. (A) Representation of model thalamocortical (TC) neuron and four terminating axons providing input to model TC neuron. (B) Oblique rectangular prism representation of the ventral intermediate (Vim) thalamus with coordinates of 50 TC model neurons randomly positioned within the nucleus. Abbreviations: CTX, cortex; RN, reticular nucleus; TIN, thalamic interneuron; CER, cerebellum; NMDA, *N*-methyl-D-aspartate; AMPA, DL-α-amino-3-hydroxy-5-methylisoxazole-4-propionic acid; GABA, γ-Aminobutyric acid
Reprinted from Birdno et al., 2012, with permission.
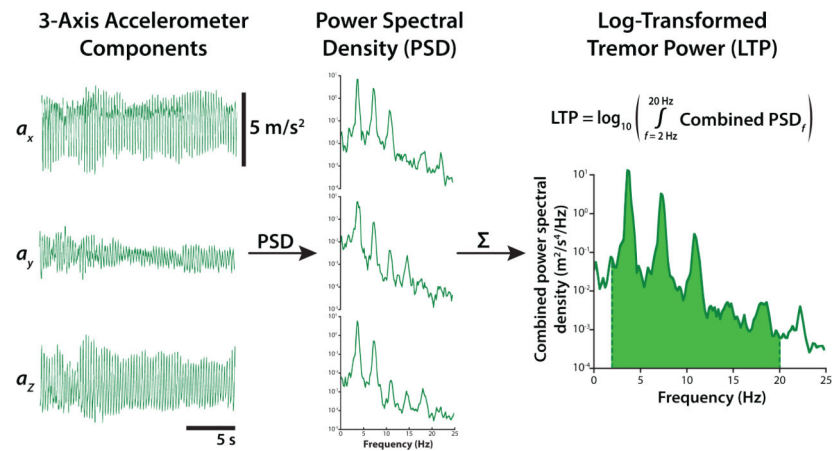
**Figure 3.**
Tremor was quantified using an accelerometer on the back of the hand. Triaxial accelerometer signals collected during a postural tremor task (*left*) and power spectra for each axis (*middle*). Spectra were summed and integrated across tremor frequencies to yield tremor power (*right*). The base 10 logarithmic transform of tremor power (LTP) is correlated with clinical ratings of tremor severity.
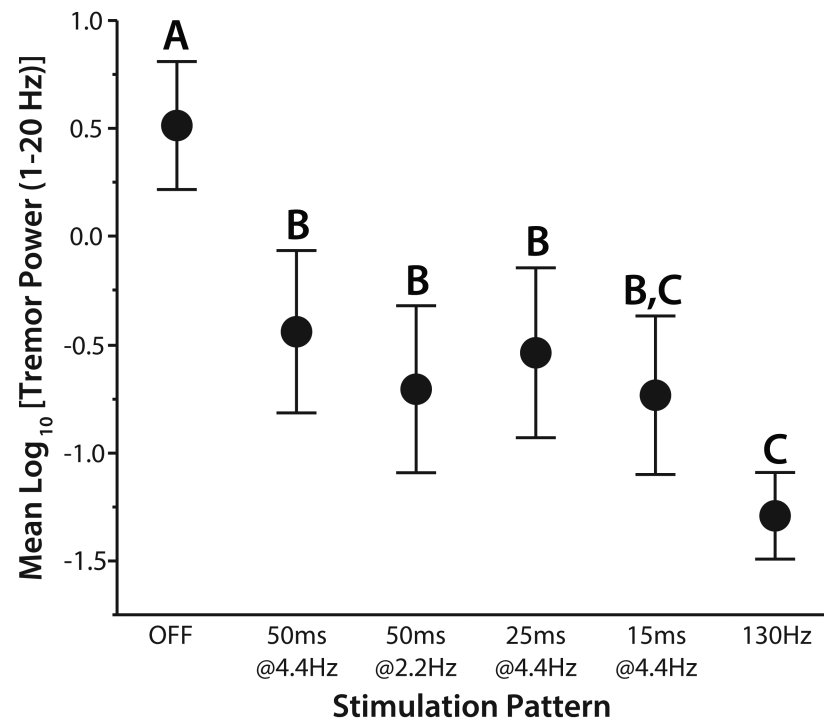
**Figure 4.**
Effects of DBS with temporal patterns of stimulation containing short pauses on postural tremor. Mean ± standard error is plotted as a function of stimulation pattern. Log-transformed tremor power (LTP) varied across stimulation patterns (F = 18.8, p<0.0001, linear mixed-effects model). Levels not sharing the same letter are significantly different (p<0.05, Tukey's HSD).
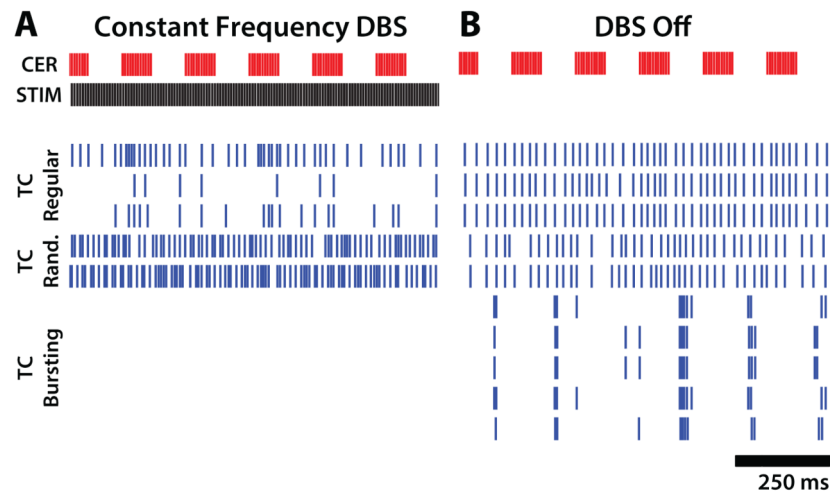
**Figure 5.**
Responses of model thalamocortical (TC) neurons to simulated DBS. Cerebellar (CER) burst-driver input and somatic firing activity for 10 of 50 model TC neurons during a one s period (A) with DBS off and (B) during 130 Hz constant frequency DBS. Rastergrams for three regular-firing, two random-firing, and five bursting-type TC cells are shown in each plot.
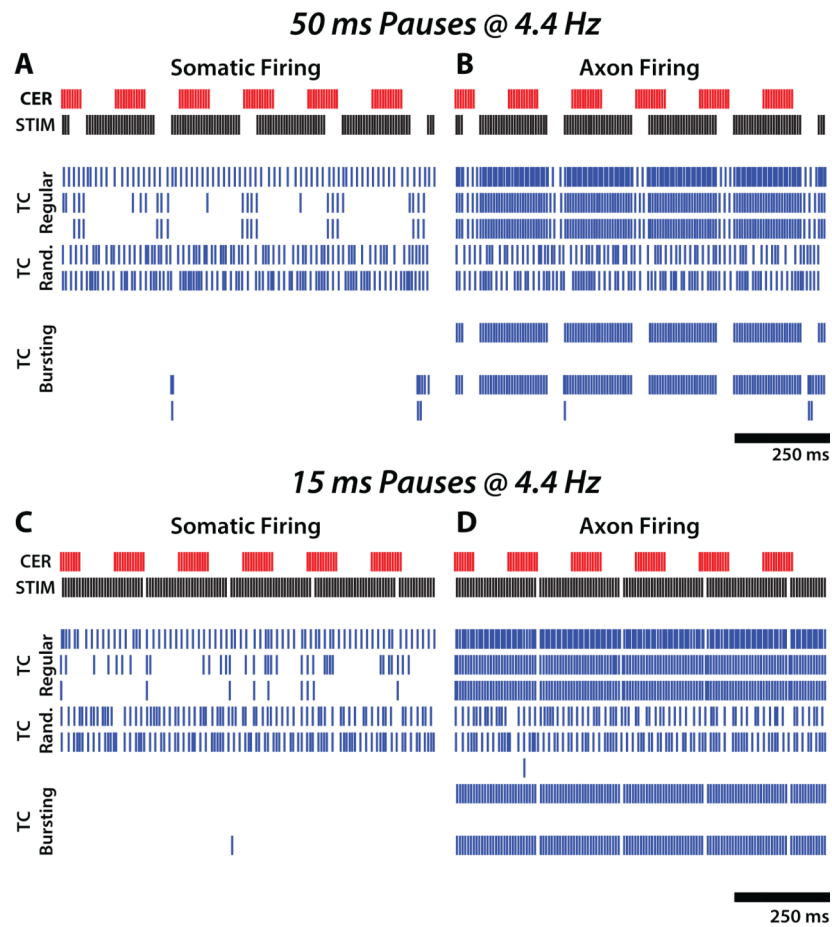
**Figure 6.**
Responses of model thalamocortical (TC) neurons to simulated pattern of DBS containing short pauses. Somatic and axonal firing pattern activity (*left* and *right* columns, respectively) for 10 representative model thalamocortical (TC) neurons during a one s of DBS with 50 or 15 ms pauses at a rate of 4.4 Hz (*top* and *bottom* rows, respectively). Rastergrams for three regular-firing, two random-firing, and five bursting-type TC cells are shown in each plot.
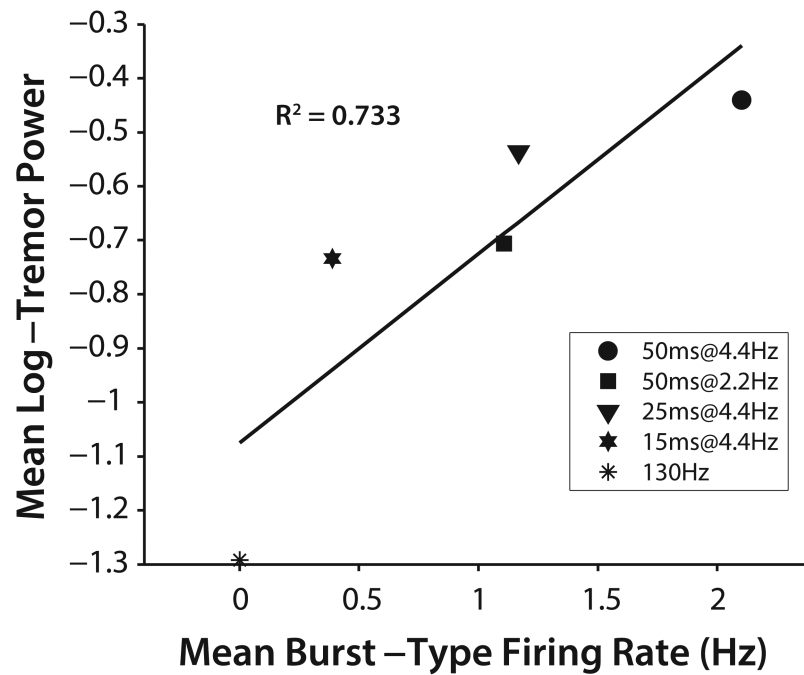
**Figure 7.**
Correlation between tremor measured in subjects with ET and thalamic DBS and mean firing rate in bursting-type model neurons across different temporal patterns of DBS ($R^2=0.733$ across stimulation conditions plotted above; $R^2=0.866$ when including stimulation OFF condition).
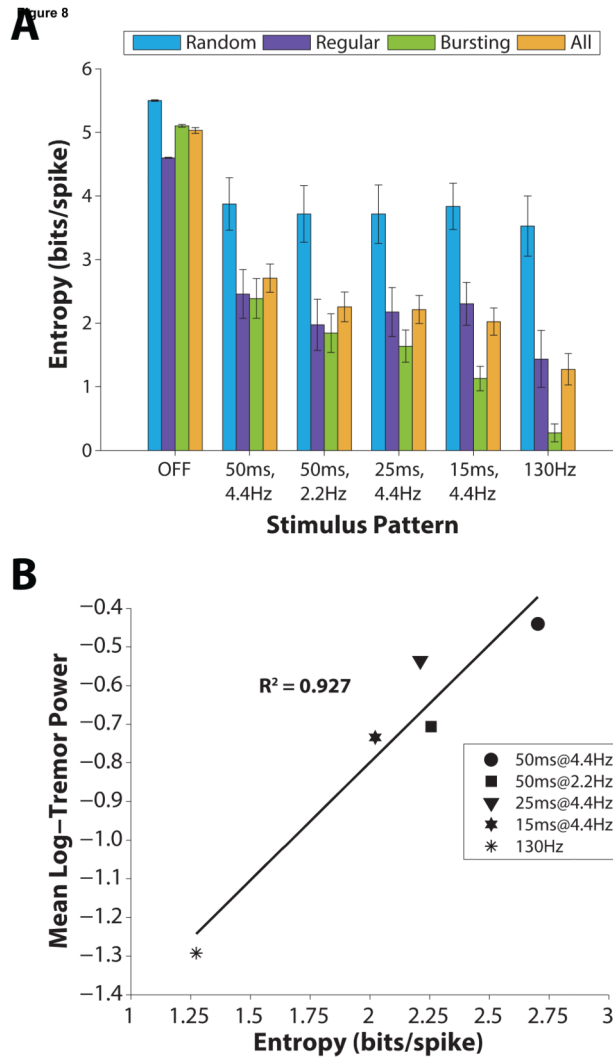
**Figure 8.**
Correlation between tremor measured in subjects with ET and thalamic DBS and firing pattern entropy of model neurons across different temporal patterns of DBS. (A) First order estimate of entropy of log-transformed interspike intervals (ISIs) for each TC neuron sub-type (*Random*, n=15; *Regular*, n=10; *Bursting*, n=25) and averaged across sub-types (*All*, n=50), reported as mean ± standard error for each stimulation pattern tested. (B) Correlation between tremor and model neuron entropy ($R^2$=0.927 across stimulation conditions plotted above; $R^2$=0.964 when including stimulation OFF condition).
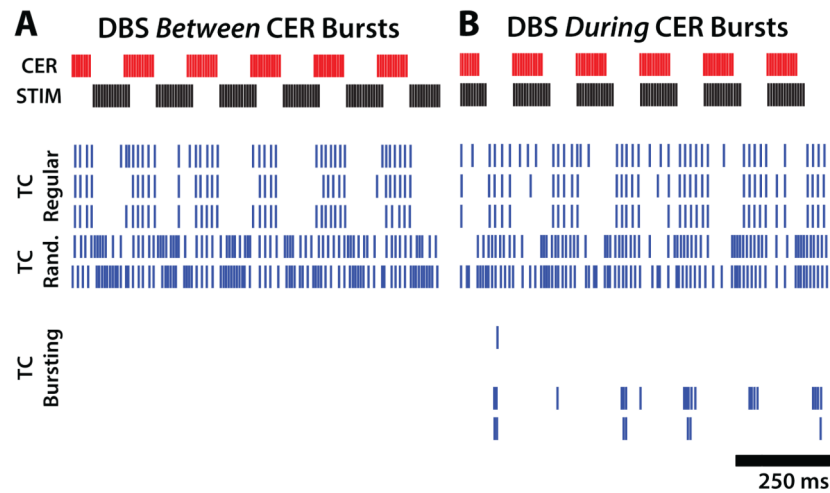
**Figure 9.**
Responses of model thalamocortical (TC) neurons to simulated patterns of cycling DBS. Cerebellar (CER) burst-driver input and somatic firing activity for 10 representative model TC neurons during a one s period with trains of 130Hz DBS triggered by the (A) beginning or (B) end of cerebellar bursts. Rastergrams for three regular-firing, two random-firing, and five bursting-type TC cells are shown in each plot.

**Table 1**

Subject demographics and clinical stimulation parameters. Experimental settings, when 544 different from clinical settings, are given in parentheses.

| ID | Age/Sex | Stimulus Contacts | PW (µs) | Amplitude (V) |
|----|---------|-------------------|---------|---------------|
| A  | 59/M    | 2+1–0–            | 150     | 3.0 (2.5)     |
| B  | 67/F    | 1+0–              | 60      | 3.6 (3.0)     |
| C  | 78/M    | 2–1–C+ (3+)       | 90      | 4.2 (6.0)     |
| D  | 85/F    | 2+0–              | 120     | 4.3           |
| E  | 69/M    | 3–2–1+            | 90      | 4.4           |
| F  | 68/M    | 1–C+ (3+)         | 90      | 4.3           |
| G  | 49/F    | 2+1–0–            | 120     | 5.6           |
| H  | 69/F    | 2+1–0–            | 90      | 4.6           |
| I  | 86/M    | 1+0–              | 90      | 3.4 (3.2)     |